

Memory-induced diffusive-superdiffusive transition: Ensemble and time-averaged observables

Adrián A. Budini

Consejo Nacional de Investigaciones Científicas y Técnicas (CONICET), Centro Atómico Bariloche, Avenida E. Bustillo Km 9.5, (8400) Bariloche, Argentina
and Universidad Tecnológica Nacional (UTN-FRBA), Fanny Newbery 111, (8400) Bariloche, Argentina
 (Received 23 February 2017; revised manuscript received 5 April 2017; published 8 May 2017)

The ensemble properties and time-averaged observables of a memory-induced diffusive-superdiffusive transition are studied. The model consists in a random walker whose transitions in a given direction depend on a weighted linear combination of the number of both right and left previous transitions. The diffusion process is nonstationary, and its probability develops the phenomenon of aging. Depending on the characteristic memory parameters, the ensemble behavior may be normal, superdiffusive, or ballistic. In contrast, the time-averaged mean squared displacement is equal to that of a normal undriven random walk, which renders the process nonergodic. In addition, and similarly to Lévy walks [Godec and Metzler, *Phys. Rev. Lett.* **110**, 020603 (2013)], for trajectories of finite duration the time-averaged displacement apparently become random with properties that depend on the measurement time and also on the memory properties. These features are related to the nonstationary power-law decay of the transition probabilities to their stationary values. Time-averaged response to a bias is also calculated. In contrast with Lévy walks [Froemberg and Barkai, *Phys. Rev. E* **87**, 030104(R) (2013)], the response always vanishes asymptotically.

DOI: 10.1103/PhysRevE.95.052110

I. INTRODUCTION

Anomalous superdiffusive processes describe a wide variety of systems arising in different disciplines such as physics and biology. Lévy walks are one of the simpler models that lead to this feature [1–6]. It is a generalization of the classical Drude model where a particle moves, in successive random directions, with constant velocity during random periods of time. Depending on the mean sojourn times a *transition* between diffusive, superdiffusive and ballistic behaviors are obtained [1,3].

Similarly to other anomalous diffusive processes [7–22], the ergodic properties of Lévy walks were recently studied [23–25]. While ensemble moments are defined in a usual way, time-averaged moments, as in single-particle tracking techniques [21], are defined by a temporal moving average performed with only one single trajectory of a given temporal length (see, for example, Refs. [7,8]):

$$\delta_\kappa(t, \Delta) \equiv \frac{\int_0^{t-\Delta} dt' [X(t'+\Delta) - X(t')]^\kappa}{t - \Delta}. \quad (1)$$

Here $X(t)$ is the walker trajectory, Δ is called the lag (or delay) time, and $\kappa = 1, 2$. For normal diffusive processes (independent random increments with a characteristic time scale), ensemble- and time-averaged moments coincide, $\lim_{t \rightarrow \infty} \delta_\kappa(t, \Delta) = \langle [X(\Delta) - X(0)]^\kappa \rangle$, a situation that defines *ergodicity*. Here $\langle \dots \rangle$ denotes ensemble average. The initial condition $X(0)$ appears due to the translational invariance of the definition (1). The so-called weak ergodicity breaking is set by the condition $\lim_{t \rightarrow \infty} \delta_\kappa(t, \Delta) \neq \langle [X(\Delta) - X(0)]^\kappa \rangle$ even for long Δ .

For Lévy walks, the behavior of the time-averaged mean square displacement [$\kappa = 2$ in Eq. (1)] strongly departs from that of subdiffusive continuous-time random walks [7,8] where, even at infinite measurement times t , they are intrinsically random objects. For Lévy walks in the *superdiffusive regime* this randomness is absent. Ensemble

and time-averaging differ only by a constant [23,24], an effect called *ultra-weak ergodicity breaking* [23]. Nevertheless, when considering trajectories made over a finite measurement time ($t < \infty$) an apparent randomness emerges both in the scaling exponents as well as in the amplitude of the time-averaged mean square displacement. This feature can be related to trajectories where the walker persists along a great fraction or even during the entire trajectory with the same velocity. On the other hand, in the *ballistic regime* an intrinsic randomness similar to that of subdiffusive processes arises when considering a shifted time-averaged moment [24]. Furthermore, time-averaged response to a bias [26,27] and a corresponding generalized Einstein relation were also studied [24,25].

The previous results were obtained from a renewal description [1] of the stochastic dynamics. Nevertheless, alternative underlying dynamics may also lead to superdiffusion. For example, similar analyses were performed by considering a deterministic diffusion model [27] and correlated random walks [28]. In addition, *globally correlated dynamics*, where the walker dynamics depends on the whole previous history of transitions [29–39], also may lead to superdiffusion. Given that the ensemble properties may be similar to those of Lévy walks it is of interest to study the ergodic properties of these strongly correlated dynamics. Added to its theoretical interest, given an experimental situation, one may obtain specific criteria for discriminating between different possible underlying nonequilibrium stochastic dynamics.

In Ref. [40] we introduced a globally correlated diffusive dynamics that leads to (ensemble) ballistic behaviors and characterized its time-averaged moments. Interestingly, the memory effects also lead to weak ergodicity breaking. Asymptotically the time-averaged moments becomes intrinsically random. The first and second moments [Eq. (1)] grow respectively linearly and quadratically with the lag time Δ . Nevertheless, the characteristic parameters of these dependences change realization to realization. A fluctuation-dissipation Einstein-like relation between the first and (a centered) second

time-averaged moments for driven and undriven dynamics respectively was also established. These features are similar to that found in Lévy walks in the ballistic regime [24]. Hence, it is natural to investigate if similar results can be obtained in a subballistic regime and to explore up to which point previous results based on renewal memoryless dynamics are intrinsic to a superdiffusive process and which are intrinsic properties of the model.

The main goal of this paper is to introduce an alternative description of superdiffusion based on global memory effects and to study its ensemble and time-averaged observables. The model interpolates between two previous known dynamics: the elephant model [29] and the urnlike model of Ref. [40]. The transition probability of the walker depends on a weighted linear combination of the number of both right and left previous transitions. Hence, jumps can be correlated or anticorrelated with the previous history. Depending on the memory parameter values, the ensemble behavior suffers a transition between diffusion, superdiffusion, and ballistic behaviors. The nonstationary character of the process is explicitly shown through its correlation. In addition, the probability evolution develops the phenomenon of aging [41–43].

We show that in contrast to Lévy walks, for infinite measurement times the time-averaged moments strongly differ from their ensemble behavior. In fact, they are equal to that of an undriven diffusion process. Hence, ergodicity is broken, while an ultraweak ergodicity breaking effect appears only in the diffusive regime. On the other hand, averages performed with finite-time trajectories develop similar properties to that of Lévy walks; that is, they become apparently random. This feature here is related to the nonstationary power-law decay of the transition probabilities to their stationary values. In contrast with previous results [24,40], for the studied model we also show that time-averaged response to a bias die out in the asymptotic regime.

The paper is outlined as follows. In Sec. II the global-correlated dynamics is introduced. A detailed characterization of its realizations is performed. In Sec. III the ensemble properties are presented (statistical moments, correlation, and probability evolution). In Sec. IV the time-averaged observables are studied. Section V is devoted to Conclusions. Analytical calculations that support the main results are presented in the appendices.

II. RANDOM WALK DYNAMICS

The model consists of a one-dimensional walker that at successive times performs random jumps. As in Refs. [29,40], both the time and position coordinates are discrete. Hence, in each discrete time step ($t \rightarrow t + \delta t$) the walker performs a jump of length δx to the right or to the left. For simplicity, time and position are measured in units of δx and δt , respectively. The stochastic position X_t at time t reads

$$X_t - X_0 \equiv x_t = \sum_{t'=1}^t \sigma_{t'}. \quad (2)$$

Here X_0 is the initial position, while x_t gives the departure with respect to it. $\sigma_t = \pm 1$ is a random variable assigned to each step. The stochastic dynamics of the variables $\{\sigma_{t'}\}_{t'=1}^t$ is as follows. At $t = 1$ (first jump or transition) the two

possible values are chosen with probability $P(\sigma_1 = \pm 1) = q_{\pm}$, where the weights satisfy $q_+ + q_- = 1$. The next values are determined by a conditional probability $\mathcal{T}(\sigma_1, \dots, \sigma_t | \sigma_{t+1})$ [the notation is such that $\mathcal{T}(A|B)$ gives the probability of B given A]. This object depends on the whole previous trajectory: $\sigma_1, \dots, \sigma_t$.

The present model relies on the selection

$$\mathcal{T}(\sigma_1, \dots, \sigma_t | \sigma_{t+1} = \pm 1) = \frac{\lambda q_{\pm} + \mu t_{\pm} + (1 - \mu)t_{\mp}}{t + \lambda}. \quad (3)$$

This transition probability depends on two free parameters, λ and μ . They satisfy the condition $\lambda \geq 0$ and $0 \leq \mu \leq 1$, respectively. Furthermore, t_+ and t_- are the number of times that the walker jumped (up to time t) to the right and to the left, respectively, $t = t_+ + t_-$.

Depending on the memory parameters λ and μ , the present model recovers two previously studied dynamics. For $\mu = 1$, the urnlike dynamics of Ref. [40] is recovered, while for $\lambda = 0$ the elephant model arises [29] (see Refs. [30,31] where this model is written in terms of the number of transitions t_{\pm}).

The parameter λ allows us to control the degree or “intensity” of the memory effects. In fact, in the limit $\lambda \rightarrow \infty$ a memoryless dynamics is recovered. On the other hand, the role of the parameter μ is to weight the two contributions t_{\pm} . For $\mu \geq 1/2$, the next jump probability is correlated (anticorrelated) with the previous trajectory. This feature can be shown by using that $t = t_+ + t_-$ and $x_t = t_+ - t_-$, which implies

$$t_{\pm} = \frac{t \pm x_t}{2}. \quad (4)$$

Hence, Eq. (3) can be rewritten as

$$\mathcal{T}(\sigma_1, \dots, \sigma_t | \sigma_{t+1} = \pm 1) = \frac{\lambda q_{\pm} + (t \pm \alpha x_t)/2}{t + \lambda}, \quad (5)$$

where for shortening the expression we defined the parameter $\alpha \equiv 2\mu - 1$. The previous equation tells us that the right-left transitions depend on the position x_t of the walker. The influence of this dependence becomes evident by considering the regime in which $t \gg \lambda$,

$$\mathcal{T}(\sigma_1, \dots, \sigma_t | \sigma_{t+1} = \pm 1) \simeq \frac{1}{2} \left(1 \pm \alpha \frac{x_t}{t} \right), \quad (6)$$

where the condition $|x_t| \leq t$ guarantees positivity. Therefore, we notice that when $\mu \geq 1/2$ ($\alpha \geq 0$), for increasing (decreasing) x_t the next jump at $t + 1$ occurs with more probability in the positive (negative) direction than in negative (positive) direction. While this dependence introduces a strong correlation along the trajectory, it is possible to demonstrate that the (random) times during which the system walks in the same direction (sojourn times) have a finite average; that is, they are not characterized by power-law statistical behaviors (see Appendix A).

A. Stationary transition probabilities

For $\mu = 1$, it is known that in the asymptotic regime ($t \gg \lambda$) the transition probability [Eq. (3)] becomes a random variable characterized by a Beta probability density [40]. On the other hand, for $\lambda = 0$ (elephant model) the previous randomness is absent. These results were demonstrated in Ref. [44] by analyzing weak ergodicity breaking in globally

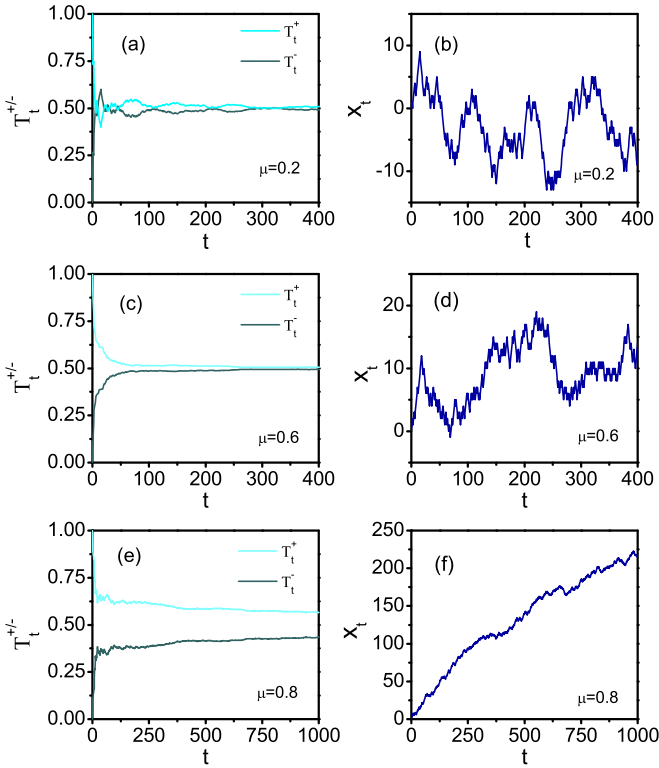


FIG. 1. Different realizations of the transition probabilities $\mathcal{T}_t^\pm = \mathcal{T}(\sigma_1, \dots, \sigma_t | \sigma_{t+1} = \pm 1)$ [Eq. (3)] jointly with the corresponding centered walker trajectory x_t [Eq. (2)] as a function of time. In all cases, $\lambda = 2$ and $q_+ = 1, q_- = 0$. The value of μ is indicated in each plot.

correlated finite systems, which in contrast to diffusive ones are endowed with a stationary state [45].

From the previous limiting behaviors, it becomes of interest to determine the stationary transition probabilities for the present model. Denoting $\mathcal{T}_t^\pm \equiv \mathcal{T}(\sigma_1, \dots, \sigma_t | \sigma_{t+1} = \pm 1)$, these quantities are $\mathcal{T}_\infty^\pm \equiv \lim_{t \rightarrow \infty} \mathcal{T}_t^\pm$, which from Eq. (3) can be written as

$$\mathcal{T}_\infty^\pm = \lim_{t \rightarrow \infty} \frac{\lambda q_\pm + \mu t_\pm + (1 - \mu)t_\mp}{t + \lambda} \quad (7a)$$

$$= \mu \lim_{t \rightarrow \infty} \frac{t_\pm}{t} + (1 - \mu) \lim_{t \rightarrow \infty} \frac{t_\mp}{t}. \quad (7b)$$

In this expression, $\lim_{t \rightarrow \infty} t_\pm/t$ are the asymptotic fraction of right-left transitions. Consistently, these values must coincide with the asymptotic transition probabilities, that is, $\mathcal{T}_\infty^\pm = \lim_{t \rightarrow \infty} t_\pm/t$. Hence, the previous equation leads to

$$\mathcal{T}_\infty^+ = \mathcal{T}_\infty^- = \frac{1}{2}, \quad 0 \leq \mu < 1, \quad (8)$$

while for $\mu = 1$ no condition for \mathcal{T}_∞^\pm is obtained. In fact, in this case $\mathcal{T}_\infty^\pm = f_\pm$, where f_\pm are Beta random variables whose probability density is $\mathcal{P}(f_\pm) = \mathcal{N}^{-1} f_+^{\lambda_+ - 1} f_-^{\lambda_- - 1}$, with $\mathcal{N} = \Gamma(\lambda_+) \Gamma(\lambda_-) / \Gamma(\lambda)$ [40,46], where $\lambda_\pm \equiv \lambda q_\pm$. Notice that Eq. (8) is equivalent to the probability transitions of a memoryless unbiased discrete diffusion process. This result is independent of the parameter λ and the weights q_\pm .

In order to check the result (8) in Fig. 1, we plot the time dependence of the transition probabilities for different values of μ , jointly with the corresponding realizations of

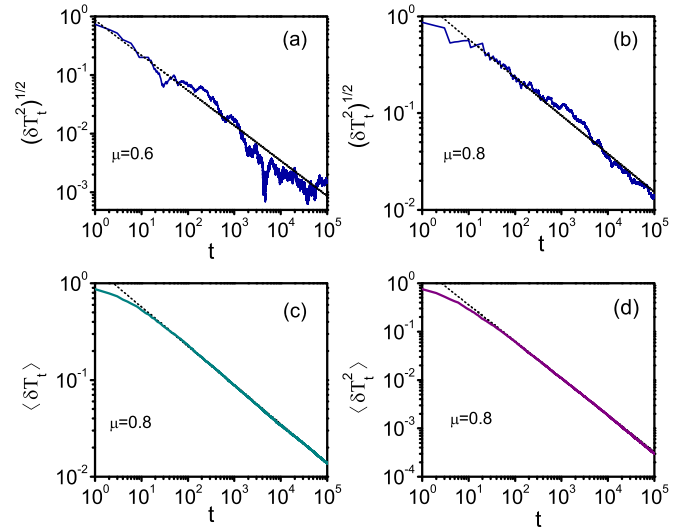


FIG. 2. Stochastic trajectories of the transition probability difference $\sqrt{\delta \mathcal{T}_t^2}$ for (a) $\mu = 0.6$ and (b) $\mu = 0.8$. In (c) and (d), the full lines correspond to the ensemble averages $\langle \delta \mathcal{T}_t \rangle$ and $\langle \delta \mathcal{T}_t^2 \rangle$ respectively. The average is performed with 200 realizations and $\mu = 0.8$. The dotted lines are power law fits, $\langle \delta \mathcal{T}_t \rangle \simeq 1.44/t^{0.40}$ and $\langle \delta \mathcal{T}_t^2 \rangle \simeq 2.07/t^{0.76}$. In all cases we take $\lambda = 2$ and $q_+ = 1, q_- = 0$.

the centered walker displacement x_t [Eq. (2)]. For $\mu = 0.2$ and $\mu = 0.6$ the transition probabilities converge in a fast way to $1/2$. Consistently, the realization of x_t looks like a standard diffusion process. On the other hand, for $\mu = 0.8$ the same asymptotic values ($1/2$) are attained. Nevertheless, the convergence is much slower. In fact, in a small time scale \mathcal{T}_t^\pm seems to attain stationary random values, a property characteristic of the case $\mu = 1$ [see Fig. 1(d) in Ref. [44]]. Due to this feature, the gap between \mathcal{T}_t^+ and \mathcal{T}_t^- drives the walker in one single direction, a property clearly seen in the trajectory of x_t .

B. Power-law convergence to the stationary transition probabilities

The plots of Fig. 1 are consistent with the asymptotic values defined by Eq. (8). On the other hand, the rate at which these values are attained strongly depend on μ . In order to characterize this property we introduce the difference $\delta \mathcal{T}_t$ between the transition probabilities

$$\delta \mathcal{T}_t \equiv \mathcal{T}_t^+ - \mathcal{T}_t^- = \frac{\lambda \delta q + \alpha(t_+ - t_-)}{t + \lambda}, \quad (9)$$

a result that follows straightforwardly from Eq. (3), where $\delta q \equiv (q_+ - q_-)$, $\delta \mathcal{T}_{t=0} = \delta q$, and as before $\alpha = (2\mu - 1)$. Notice that $\delta \mathcal{T}_t$ can be read as the *instantaneous drift* felt by the walker.

In Figs. 2(a) and 2(b) we plot $\sqrt{\delta \mathcal{T}_t^2}$. We find that, after an initial transient, independently of the parameter values of the model, $\sqrt{\delta \mathcal{T}_t^2} \approx c/t^\beta$, where c and β change in each realization. As shown by the figures, this behavior is valid over many decades of time. For $\mu < 1/2$ (not shown) the signal $\sqrt{\delta \mathcal{T}_t^2}$ becomes more noisy [see Fig. 1(a)], but a power-law decay behavior is also present.

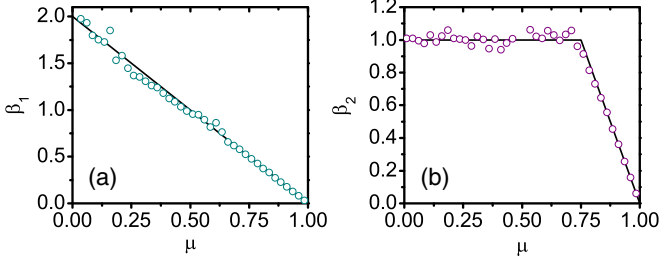


FIG. 3. Dependence with the parameter μ of the scaling exponents (a) β_1 and (b) β_2 corresponding to the ensemble averages $\langle \delta T_t \rangle$ and $\langle \delta T_t^2 \rangle$, respectively [Eq. (10)]. The circles were obtained from numerical simulations [see Figs. 2(c) and 2(d)], while the full lines gives their fit [Eqs. (11) and (12)].

In order to characterize the previous decay behaviors in Fig. 2(c) and 2(d) we plot $\langle \delta T_t \rangle$ and $\langle \delta T_t^2 \rangle$ for the same value of μ . Here $\langle \dots \rangle$ denotes average over an ensemble of realizations. For both quantities we find that asymptotically a power-law fitting always applies

$$\langle \delta T_t \rangle \simeq \frac{c_1}{t^{\beta_1}}, \quad \langle \delta T_t^2 \rangle \simeq \frac{c_2}{t^{\beta_2}}. \quad (10)$$

The time scale where this fitting start to be valid strongly depend on μ . Nevertheless, when achieved, we found that the scaling exponents β_1 and β_2 depend only on the parameter μ .

C. Memory-induced transition

A (memory-induced) transition is found when analyzing the dependences of the scaling exponents β_1 and β_2 with the parameter μ . They can be determinate in a numerical way [see Figs. 2(c) and 2(d)], results shown in Fig. 3. The scaling exponents can be fit as

$$\beta_1 = 2(1 - \mu), \quad (11)$$

while for the second moment as ($\mu \neq 1/2$, $\mu \neq 1$)

$$\beta_2 = \begin{cases} 4(1 - \mu) & \text{if } 3/4 \leq \mu < 1 \\ 1 & \text{if } 0 \leq \mu \leq 3/4 \end{cases}. \quad (12)$$

While β_1 presents a monotonous linear behavior, the dependence of β_2 with μ suffers a transition at $\mu = 3/4$. This is an intrinsic property of the correlation mechanism defined by the transition probability (3), which in turn is independent of the parameters λ and q_{\pm} .

For β_2 two values of μ are not described by Eq. (12). First, for $\mu = 1$, δT_t converges to $\lim_{t \rightarrow \infty} \delta T_t = f_+ - f_-$, where f_{\pm} are Beta random variables that in each realization satisfy $f_{\pm} \neq 1/2$ [40]. Therefore, in this case the exponent β_2 [Eq. (10)] loses its meaning.

For $\mu = 1/2$, from Eq. (9) [with $\alpha = 0$] it follows the deterministic behavior $\delta T_t = \lambda \delta q / (t + \lambda)$, leading to $\beta_1 = 1$ and $\beta_2 = 2$. Hence, this value of β_2 is not covered by the fitting (12). Numerically, we checked that this is the only exception. Consistently, we found that around this point ($\mu \simeq 1/2$) the $1/t^{\beta_2}$ power-law decay of $\langle \delta T_t^2 \rangle$ occurs at higher times. These properties and results are supported by analytical calculations presented in next sections.

D. Relation between average transition fluctuations and walker ensemble properties

The memory-induced transition defined from the asymptotic decay of $\langle \delta T_t^2 \rangle$ is analytically demonstrated in the next section by studying the ensemble properties of the random walker trajectories. In fact, each trajectory of δT_t [Eq. (9)], given that $x_t = t_+ - t_-$, can be written as $\delta T_t = (\lambda \delta q + \alpha x_t) / (t + \lambda)$. Hence,

$$\langle \delta T_t \rangle = \frac{\lambda \delta q + \alpha \langle x_t \rangle}{t + \lambda}, \quad (13)$$

while the second moment becomes

$$\langle \delta T_t^2 \rangle = \langle \delta T_t \rangle^2 + \frac{\alpha^2 [\langle x_t^2 \rangle - \langle x_t \rangle^2]}{(t + \lambda)^2}. \quad (14)$$

Furthermore, defining $\tilde{\delta T}_t = \delta T_t - \langle \delta T_t \rangle$, it follows that

$$\langle \tilde{\delta T}_{t+\tau} \tilde{\delta T}_t \rangle = \frac{\alpha^2 [\langle x_{t+\tau} x_t \rangle - \langle x_{t+\tau} \rangle \langle x_t \rangle]}{(t + \tau + \lambda)(t + \lambda)}. \quad (15)$$

The previous relations demonstrate that the statistical properties of δT_t and those of x_t can be put in one-to-one correspondence. This relation is also valid for the variable σ_t , which can be read as the “walker velocity.” Given that T_t^{\pm} gives the probability for $\sigma_{t+1} = \pm 1$, it follows

$$\langle \sigma_{t+1} \rangle = \langle \delta T_t \rangle, \quad \langle \sigma_{t+1}^2 \rangle = 1. \quad (16)$$

On the other hand, defining the centered velocity $\tilde{\sigma}_t \equiv \sigma_t - \langle \sigma_t \rangle$, its correlation reads

$$\langle \tilde{\sigma}_{t+\tau+1} \tilde{\sigma}_{t+1} \rangle = \langle \tilde{\delta T}_{t+\tau} \tilde{\delta T}_t \rangle. \quad (17)$$

Therefore, the properties of σ_t can also be determined from the ensemble behavior of x_t .

III. ENSEMBLE PROPERTIES

In this section we study the ensemble properties (moments and correlation) of the random walk defined by Eq. (3). They not only determine the moments of the transition probability difference δT_t , but also set the behavior of the time-averaged observables (next section). The probability of finding the walker at a given time is also obtained.

The walker statistical moments can be obtained in an exact analytical way by introducing the double characteristic function

$$Q(k_1, t; k_2, \tau) \equiv \langle \exp[i(k_1 x_t + k_2 x_{t+\tau})] \rangle. \quad (18)$$

In Appendix B we obtain an explicit recurrence relation for this object. As usual, recursive relations for the moments follow by differentiation with respect to k_1 and k_2 . Below, we also provide the corresponding exact solutions. Numerical simulations support the following analytical results.

A. First moment

For the *first moment*, it follows the recursive relation

$$\langle x_{t+1} \rangle = \langle x_t \rangle \left[1 + \frac{\alpha}{t + \lambda} \right] + \frac{\lambda}{t + \lambda} \delta q, \quad (19)$$

$\alpha = 2\mu - 1$. Notice that for $\lambda \neq 0$, the factor $\delta q = q_+ - q_-$ can be read as an external bias that drifts the average dynamics.

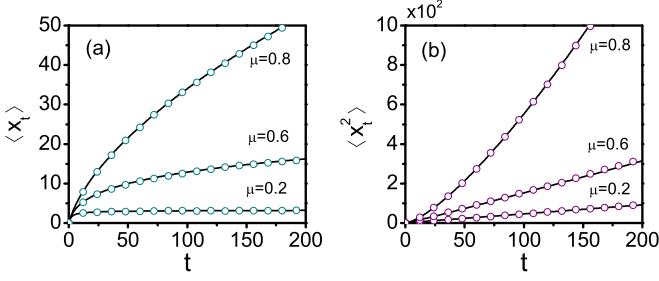


FIG. 4. Ensemble moments of the random walker. (a) First moment $\langle x_t \rangle$. (b) Second moment $\langle x_t^2 \rangle$. The full lines correspond to the exact expressions (20) and (23), respectively. In (a) we take $q_+ = 1, q_- = 0$, while in (b) $q_+ = q_- = 1/2$. In all cases $\lambda = 2$. The value of μ is indicated in each curve. Numerical results (circles) were obtained from an average over 5×10^3 realizations.

The solution of the previous equation is

$$\langle x_t \rangle = \frac{\delta q}{\alpha} \left[\frac{\Gamma(\lambda + 1) \Gamma(\alpha + \lambda + t)}{\Gamma(\alpha + \lambda) \Gamma(\lambda + t)} - \lambda \right], \quad (20)$$

where $\Gamma(z)$ is the Gamma function. For $\mu = 1/2$, that is, $\alpha = 0$, it follows $\langle x_t \rangle = \delta q \lambda [\psi(\lambda + t) - \psi(\lambda)]$, where the digamma function is defined as $\psi(z) = (d/dz) \ln[\Gamma(z)]$. At $\mu = 1$, $\langle x_t \rangle = \delta q t$.

In the long time limit, $t \gg \lambda$, by using the approximation $\Gamma(z + v)/\Gamma(z) \simeq z^v$ valid for $z \rightarrow \infty$, from Eq. (20) we get the asymptotic behaviors

$$\langle x_t \rangle \approx \begin{cases} \frac{\delta q}{(2\mu-1)} \frac{\Gamma(\lambda+1)}{\Gamma(2\mu-1+\lambda)} t^{(2\mu-1)} & \mu > 1/2, \\ \delta q \lambda \ln(t) & \mu = 1/2, \\ \frac{\delta q \lambda}{(1-2\mu)} & \mu < 1/2. \end{cases} \quad (21)$$

By taking into account these asymptotic behaviors, from Eqs. (13) and (20) it is possible to confirm the fitting for β_1 given by Eq. (11).

For $\delta q = q_+ - q_- \neq 0$ the first moment grows indefinitely with time when $\mu \geq 1/2$ and saturates to a constant value when $\mu < 1/2$. In order to check these properties, in Fig. 4(a) we plot $\langle x_t \rangle$ obtained from an ensemble of stochastic realizations such as those shown in Fig. 1. Theoretical and numerical results are indistinguishable in the scale of the plots.

The different behaviors shown in Fig. 4(a) are a consequence of the power-law decay of $\delta \mathcal{T}_t$ to its stationary value, $\lim_{t \rightarrow \infty} \delta \mathcal{T}_t = 0$ [see Eq. (8)]. In fact, from the dependence of the exponent β_1 with parameter μ [Eq. (11)] and the relation between $\langle \delta \mathcal{T}_t \rangle$ and $\langle x_t \rangle$ [Eq. (13)], which can be rewritten as $\alpha \langle x_t \rangle = \langle \delta \mathcal{T}_t \rangle (t + \lambda) - \lambda \delta q$, it follows that the first moment grows in time only for $\mu \geq 1/2$.

B. Second moment

For the *second moment*, we get the recursive relation

$$\langle x_{t+1}^2 \rangle = \langle x_t^2 \rangle \left[1 + \frac{2\alpha}{t + \lambda} \right] + 1 + 2\delta q \frac{\lambda}{t + \lambda} \langle x_t \rangle, \quad (22)$$

whose solution is given by

$$\langle x_t^2 \rangle = \frac{1}{2\alpha - 1} \left[\frac{\Gamma(\lambda + 1) \Gamma(2\alpha + \lambda + t)}{\Gamma(2\alpha + \lambda) \Gamma(\lambda + t)} - (n + \lambda) \right] + \varphi(t), \quad (23)$$

where $2\alpha - 1 = 4\mu - 3$. The bracket term gives the solution when $\delta q = 0$, while $\varphi(t)$ takes into account the contributions proportional to $\delta q \neq 0$,

$$\varphi(t) \equiv \delta q^2 \lambda^2 \left\{ 1 + \frac{\Gamma(\lambda) \left[\frac{\Gamma(\lambda + 2\alpha + t)}{\Gamma(\lambda + 2\alpha)} - \frac{2\Gamma(\lambda + \alpha + t)}{\Gamma(\lambda + \alpha)} \right]}{\Gamma(t + \lambda)} \right\}. \quad (24)$$

In the long time limit, $t \gg \lambda$, by using the approximation $\Gamma(z + v)/\Gamma(z) \simeq z^v$ valid for $z \rightarrow \infty$, in the case $\delta q = 0$ we get the asymptotic behaviors

$$\langle x_t^2 \rangle \approx \begin{cases} \frac{1}{4\mu-3} \frac{\Gamma(\lambda+1)}{\Gamma(4\mu-2+\lambda)} t^{4\mu-2} & \mu > 3/4, \\ t \ln(t) & \mu = 3/4, \\ \frac{t}{3-4\mu} & \mu < 3/4. \end{cases} \quad (25)$$

By introducing these behaviors in Eq. (14) it is possible to recover analytically the fitting for β_2 [Eq. (12)]. In fact, corrections proportional to $\langle x_t \rangle$ and $\varphi(t)$, Eqs. (21) and (24) respectively, gives higher order (inverse) power-law corrections that can be disregarded in the asymptotic regime.

We notice that $\langle x_t^2 \rangle$ [Eq. (25)] develops a transition between a *normal diffusive behavior* ($\mu < 3/4$) to a *superdiffusive one* ($\mu > 3/4$). These features are related to the exponent β_2 of the power-law decay of $\langle \delta \mathcal{T}_t^2 \rangle$ [Eqs. (10) and (14)]. In Fig. 4(b) we plot $\langle x_t^2 \rangle$ for different values of μ . Numerical simulations confirm the theoretical predictions. On the other hand, at $\mu = 1$, a *ballistic behavior* is obtained asymptotically, $\langle x_t^2 \rangle = t(t + \lambda)/(1 + \lambda)$, a result derived in Ref. [40].

C. Correlation

The correlation of the random walker is defined as

$$C_{t,\tau}^x \equiv \langle x_t x_{t+\tau} \rangle, \quad (26)$$

with initial condition $C_{t,0}^x = \langle x_t^2 \rangle$. From the double characteristic function (Appendix B), it is possible to obtain the recursive relation

$$C_{t,\tau+1}^x = C_{t,\tau}^x \left[1 + \frac{\alpha}{t + \tau + \lambda} \right] + \frac{\lambda \delta q}{t + \tau + \lambda} \langle x_t \rangle. \quad (27)$$

Its solution is

$$C_{t,\tau}^x = \left[\langle x_t^2 \rangle + \frac{\lambda \delta q}{\alpha} \langle x_t \rangle \right] \Phi(t, \tau) - \frac{\lambda \delta q}{\alpha} \langle x_t \rangle, \quad (28)$$

where $\langle x_t \rangle$ and $\langle x_t^2 \rangle$ follow from Eqs. (20) and (23), respectively. The auxiliary function $\Phi(t, \tau)$ reads

$$\Phi(t, \tau) \equiv \frac{\Gamma(\lambda + t) \Gamma(\alpha + \lambda + t + \tau)}{\Gamma(\alpha + \lambda + t) \Gamma(\lambda + t + \tau)}. \quad (29)$$

For $\mu = 1/2$, that is, $\alpha = 0$, the solution of the recursive relation (27) reads as $C_{t,\tau}^x = \langle x_t^2 \rangle + \langle x_t \rangle \lambda \delta q [\psi(\lambda + t + \tau) - \psi(t + \tau)]$, where the digamma function is defined as $\psi(z) = (d/dz) \log \Gamma(z)$. In the limit $\mu \rightarrow 1$, $C_{t,\tau}^x$ is given by Eq. (28) with $\Phi(t, \tau) = [1 + \tau/(t + \lambda)]$.

In the asymptotic regime, by using the approximation $\Gamma(z + v)/\Gamma(z) \simeq z^v$, valid for $z \rightarrow \infty$, it follows $\Phi(t, \tau) \simeq$

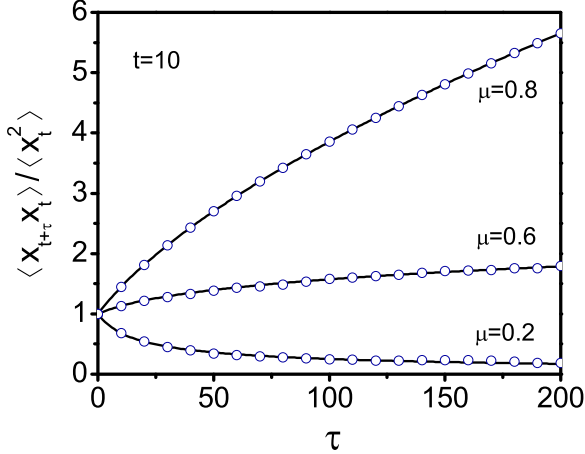


FIG. 5. Normalized correlation $\langle x_{t+\tau} x_t \rangle / \langle x_t^2 \rangle$ as a function of the difference time τ . The full lines correspond to the exact result Eq. (28). In all cases we take $t = 10$, $q_+ = q_- = 1/2$, and $\lambda = 2$. The value of μ is indicated in each curve. Numerical results (circles) were obtained from an average over 2×10^4 realizations.

$[1 + \tau/(t + \lambda)]^\alpha$, which leads to

$$C_{t,\tau}^x \simeq \left[\langle x_t^2 \rangle + \frac{\lambda \delta q}{\alpha} \langle x_t \rangle \right] \left(1 + \frac{\tau}{t} \right)^\alpha - \frac{\lambda \delta q}{\alpha} \langle x_t \rangle. \quad (30)$$

Thus, in the asymptotic regime the correlation depends on the quotient (τ/t) , showing the strong nonstationarity property of the diffusion process. A similar result is also valid for Lévy walks [24]. On the other hand, for $\mu \geq 1/2$ (equivalently $\alpha \geq 0$) $C_{t,\tau}^x$ increases (decreases) with τ . This result is consistent with the correlation-anticorrelation mechanism introduced by μ . In order to check these results, in Fig. 5 we plot the normalized correlation $\langle x_{t+\tau} x_t \rangle / \langle x_t^2 \rangle$ as a function of the interval τ . Numerical simulations and analytical results are indistinguishable in the scale of the plots.

D. Joint-probability evolution

By Fourier inversion, $k_1 \rightarrow y$, $k_2 \rightarrow x$, the double characteristic function (18) also allows us to obtain the joint probability $P(y, t; x, \tau)$ of observing the walker at position y at time t and at position x at time $t + \tau$. From Eq. (B6) we get

$$P(y, t; x, \tau + 1) = W_{t,\tau}^+(x - 1)P(y, t; x - 1, \tau) + W_{t,\tau}^-(x + 1)P(y, t; x + 1, \tau), \quad (31)$$

where the transition probabilities are

$$W_{t,\tau}^\pm(x) = \frac{1}{2} \left[1 \pm \frac{1}{t + \tau + \lambda} (\alpha x + \lambda \delta q) \right]. \quad (32)$$

Hence, the dynamics as a function of the interval τ develops aging [41–43]; that is, here the transition probabilities $W_{t,\tau}^\pm(x)$ depend on the starting time t with a power-law dependence. This property is closely related with the asymptotic power-law behavior of the walker correlation [Eq. (30)]. These features are absent in the memoryless limit, $\lim_{\lambda \rightarrow \infty} W_{t,\tau}^\pm(x) = q_\pm$.

In a continuous limit, where both the jump length δx and the time interval δt between consecutive transitions become

small, the previous master equation leads to the Fokker-Planck equation

$$\begin{aligned} \frac{\partial}{\partial \tau} P(y, t; x, \tau) &= D \frac{\partial^2}{\partial x^2} P(y, t; x, \tau) \\ &- \frac{\alpha}{t + \tau + t_\lambda} \frac{\partial}{\partial x} [x P(y, t; x, \tau)] \\ &- \frac{t_\lambda}{t + \tau + t_\lambda} V \frac{\partial}{\partial x} P(y, t; x, \tau), \end{aligned}$$

where the parameters are $D \equiv (1/2)\delta x^2/\delta t$, $V \equiv (q_+ - q_-)(\delta x/\delta t)$, and $t_\lambda \equiv \lambda \delta t$. Interestingly, this equation has the form of a diffusion process in a time- and age- (power-law) dependent inverted parabolic potential superimposed with a time-dependent linear drift. Notice that around $\mu = 1/2$ the potential is inverted, property related to the correlation-anticorrelation mechanism introduced by the parameter μ .

IV. TIME-AVERAGED OBSERVABLES

Here we study the ergodic properties of the walker defined by Eq. (3). Given the discrete nature of the dynamics, the definition of the time-averaged moments is given by

$$\delta_k(t, \Delta) = \frac{\sum_{t'=0}^{t-\Delta} [x(t' + \Delta) - x(t')]^k}{t - \Delta}. \quad (33)$$

Here we have used the translational invariance of Eq. (1), which allows us to write the definition in terms of $x(t)$ [Eq. (2)]. The definitions of ergodicity and ergodicity breaking are those quoted in the Introduction.

A. Infinite-time trajectories

The walker ensemble properties are mainly determinate by the decay behavior of the transition probabilities. In contrast, for infinite-time trajectories, $\lim_{t \rightarrow \infty} \delta_k(t, \Delta)$, the time-averaged moments are settled by the asymptotic behavior of the transition probabilities. In fact, taking higher times t in Eq. (33), the relevant walker transitions are those governed by the asymptotic values $\mathcal{T}_\infty^\pm = 1/2$ [Eq. (8)]. Consequently, we expect that along a single trajectory the time-averaged moments of x_t converge to those of an undriven normal diffusion process. Hence, it follows

$$\lim_{t \rightarrow \infty} \delta_1(t, \Delta) = 0, \quad 0 \leq \mu < 1, \quad (34)$$

while the time-averaged mean square displacement reads

$$\lim_{t \rightarrow \infty} \delta_2(t, \Delta) = \Delta, \quad 0 \leq \mu < 1. \quad (35)$$

For normal diffusion, these expressions follows straightforwardly from the definition (33) and by considering independent random walker increments.

The previous results imply that the process is not ergodic. In fact, $\langle x_\Delta \rangle \neq \lim_{t \rightarrow \infty} \delta_1(t, \Delta)$, and $\langle x_\Delta^2 \rangle \neq \lim_{t \rightarrow \infty} \delta_2(t, \Delta)$. These inequalities remain valid even for $\Delta \gg 1$ [see Eqs. (21) and (25) respectively] and are valid for any value of λ , μ , and q_\pm .

Interestingly, while the bias induced by $\delta q = q_+ - q_-$ drives the ensemble behavior [see Eq. (21)], the time-averaged response [$\lim_{t \rightarrow \infty} \delta_1(t, \Delta)$] vanishes (dye out) asymptotically [Eq. (34)]. In consequence, it is not possible to ask about

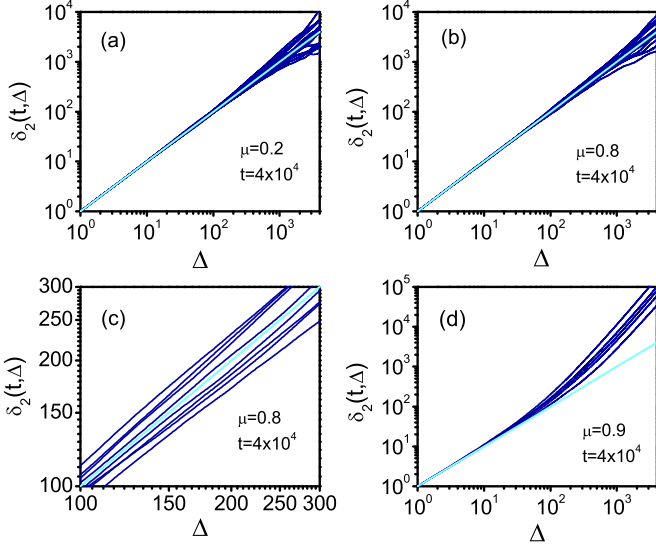


FIG. 6. Dependence with the lag time Δ of the time-averaged mean square displacement $\delta_2(t, \Delta)$ obtained for different walker trajectories [see Fig. 1]. The gray lines (light blue lines) correspond to the infinite trajectory limit, $\lim_{t \rightarrow \infty} \delta(t, \Delta) = \Delta$. In (a) (25 trajectories) we take $\mu = 0.2$. In (b) (25 trajectories) $\mu = 0.8$. In (c) a few of the previous trajectories are shown in the time scale posterior to the linear regime. In (d) (5 trajectories) $\mu = 0.9$. In all cases, we take $\lambda = 2$, $q_+ = q_- = 1/2$, and $t = 4 \times 10^4$.

an Einstein fluctuation dissipation relation formulated with time-averaged observables (infinite-time trajectories). This unusual property relies on both the power-law decay of the transitions probabilities and their stationary on-half values.

While for the second moment time and ensemble averages are always different, when $\mu < 3/4$ [diffusive-like regime; Eq. (25)] they differ only in terms of a constant, $\lim_{t \rightarrow \infty} \delta_2(t, \Delta)/(3 - 4\mu) = \Delta/(3 - 4\mu) \simeq \langle x_\Delta^2 \rangle$. In contrast, for Lévy walks this ultraweak ergodicity breaking is valid in the superdiffusive regime.

In order to check these results, in Fig. 6 we plot a set of realizations corresponding to $\delta_2(t, \Delta)$ for different values of μ . Around the origin all realizations approach the limit defined by Eq. (35). We checked that by increasing the measurement time t , the departure with respect to the linear behavior consistently occurs at larger delay times Δ .

B. Randomness in finite-time trajectories

The previous results are valid for any (finite) value of λ and $0 \leq \mu < 1$. When $\mu = 1$, the model reduces to the urnlike dynamics of Ref. [40]. Thus,

$$\lim_{t \rightarrow \infty} \delta_1(t, \Delta) = (f_+ - f_-)\Delta, \quad (36)$$

while the second time-averaged moment reads

$$\lim_{t \rightarrow \infty} \delta_2(t, \Delta) = (f_+ - f_-)^2 \Delta^2 + [1 - (f_+ - f_-)^2] \Delta, \quad (37)$$

where f_\pm are Beta random variables, with $f_+ + f_- = 1$ [see Eqs. (32) and (33) in Ref. [40] where these results were derived]. The transition between these scaling and those defined by Eqs. (34) and (35) can be described by analyzing

the behavior of the time-averaged moments obtained with finite-time trajectories.

In the plots of Fig. 6 we observe that, even when $\Delta \ll t$, beyond the linear regime the scaling of $\delta_2(t, \Delta)$ can be subdiffusive or superdiffusive. Furthermore, the amplitude of the scaling can also be random [see Fig. 6(c)]. These properties also arise in Lévy walks [23]. Here these features are present for all values of μ . Hence, we associate these effects to the random behavior of the transition probabilities (see Figs. 1 and 2). In fact, independently of the values of the memory parameters μ and λ , they decay to their stationary values following a power-law behavior with parameters that are intrinsically random [see Eqs. (9) and (10)]. For $\mu \approx 1$, all realizations become superdiffusive [see Fig. 6(d), $\mu = 0.9$], a consistent property necessary for approaching the scaling defined by Eq. (37).

C. Ensemble average of finite-time trajectories

Now we study how the finiteness of single trajectories affects the corresponding average over an ensemble of trajectories. From Eq. (33) the first moment reads

$$\langle \delta_1(t, \Delta) \rangle = \frac{1}{t - \Delta} \sum_{t'=0}^{t-\Delta} \langle x_{t'+\Delta} \rangle - \langle x_{t'} \rangle, \quad (38)$$

while the second one can be written as

$$\langle \delta_2(t, \Delta) \rangle = \frac{1}{t - \Delta} \sum_{t'=0}^{t-\Delta} \langle x_{t'+\Delta}^2 \rangle + \langle x_{t'}^2 \rangle - 2 \langle x_{t'+\Delta} x_{t'} \rangle. \quad (39)$$

Given the exact analytical expressions for $\langle x_t \rangle$ [Eq. (20)], $\langle x_t^2 \rangle$ [Eq. (23)], and the correlation $\langle x_{t'+\Delta} x_{t'} \rangle$ [Eq. (28)], we can also evaluate these objects in an exact way. Nevertheless, they cannot be expressed in terms of general simple expressions. Only for special values can one get simpler ones. For example, for $\mu = 1$ Eq. (38) becomes

$$\langle \delta_1(t, \Delta) \rangle = \delta q \Delta \left[1 + \frac{1}{t - \Delta} \right], \quad \mu = 1. \quad (40)$$

Taking $\delta q = q_+ - q_- = 0$, the mean square displacement [Eq. (39)] reads

$$\langle \delta_2(t, \Delta) \rangle = \frac{\Delta(\Delta + \lambda)}{1 + \lambda} \left[1 + \frac{1}{t - \Delta} \right], \quad \mu = 1. \quad (41)$$

In the limit $t \rightarrow \infty$, these expressions correspond to the average over realizations of Eqs. (36) and (37) (see Ref. [40]). On the other hand, the finite-time effects are given by the contributions proportional to $1/(t - \Delta)$.

For $\mu < 1$, given that simple analytical expressions cannot be obtained, in Appendix C we introduce a set of approximations that allow us to obtain the asymptotic behavior ($t \gg \Delta$) of the exact expressions Eqs. (38) and (39). We get

$$\langle \delta_1(t, \Delta) \rangle \sim \delta q c_0 \left\{ \frac{2\mu\Delta}{t^{2(1-\mu)}} - \frac{1}{t} [(\Delta + \lambda)^{2\mu} - \lambda^{2\mu}] \right\}, \quad (42)$$

where $c_0 = \Gamma(\lambda + 1)/[2\mu\alpha\Gamma(\alpha + \lambda)]$. Consistently with Eq. (34), $\langle \delta_1(t, \Delta) \rangle$ vanishes when $t \rightarrow \infty$. This regime is approached following a power-law behavior. In fact, for $\mu < 1/2$, $\langle \delta_1(t, \Delta) \rangle \sim \Delta^{2\mu}/t$, while for $\mu > 1/2$, $\langle \delta_1(t, \Delta) \rangle \sim \Delta/t^{2(1-\mu)}$.

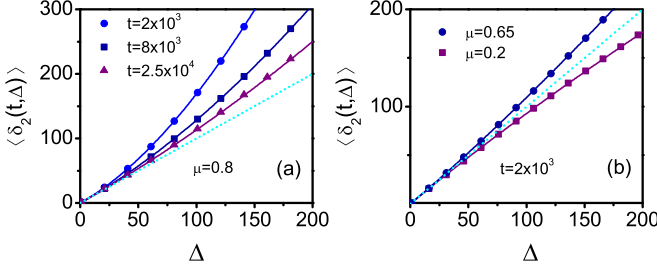


FIG. 7. Ensemble average $\langle \delta_2(t, \Delta) \rangle$ as a function of Δ . In (a) we take $\mu = 0.8$, and three different times, $t = 2 \times 10^3$ (circles), $t = 8 \times 10^3$ (squares), and $t = 25 \times 10^3$ (triangles). In (b) we take $t = 2 \times 10^3$ and $\mu = 0.65$ (circles), $\mu = 0.2$ (squares). The full lines correspond to the fitting (43) valid for large times. The dotted lines give the infinite trajectory limit, $\lim_{t \rightarrow \infty} \langle \delta_2(t, \Delta) \rangle = \Delta$. The numerical results (circles, squares, triangles) were obtained from an average over 2×10^3 realizations.

Taking $\delta q = q_+ - q_- = 0$, for the mean squared displacement we obtain

$$\langle \delta_2(t, \Delta) \rangle \sim \Delta + \frac{\Delta^2}{t} \left[a + b \ln \left(\frac{\Delta}{t} \right) \right] + c \frac{\Delta^2}{t^{4(1-\mu)}} + d \frac{\Delta^{4\mu-1}}{t}, \quad (43)$$

where a , b , c , and d are constants given in Appendix C. The factor proportional to d only contributes for $\mu > 1/2$.

In Eq. (43), the deviations with respect to the linear behavior (35) change around $\mu = 3/4$. For $\mu < 3/4$, the dominant terms are those proportional to a and b , while for $\mu > 3/4$ are those proportional to c and d . In fact, the quadratic contribution Δ^2 dominates at $\mu = 1$, which approximate the exact behavior (41).

In contrast to Lévy walks [see Eq. (18) In Ref. [24]], by comparing the asymptotic behaviors of $\langle \delta_1(t, \Delta) \rangle$ [Eq. (42)] and $\langle \delta_2(t, \Delta) \rangle$ [Eq. (43)] we conclude that, for finite-time trajectories, it is not possible to establishing a simple relation between both objects (an Einstein-like relation).

In order to check the previous results, in Fig. 7(a) we plot $\langle \delta_2(t, \Delta) \rangle$ for different times and the same μ . An increasing convergence to the lineal regime, $\langle \delta_2(t, \Delta) \rangle \simeq \Delta$, is observed for increasing t . In Fig. 7(b) we plot $\langle \delta_2(t, \Delta) \rangle$ for different values of μ . For $\mu < 1/2$ it is a concave function of Δ while it is convex for $\mu > 1/2$. In all plots, the numerical results, the exact result (39), and the approximation (43) are indistinguishable in the scale of the graphs.

V. SUMMARY AND CONCLUSIONS

The studied model consists of a diffusive walker whose successive jumps depend on the whole previous history of transitions [Eq. (3)]. The second moment develops a diffusive-superdiffusive transition. This memory-induced property can be directly related to a transition in the power-law decay behavior of the transition probabilities to their stationary values (see Figs. 1 to 3), which in fact develop a similar transition for the same parameter values [see Eqs. (12) and (25)]. The ensemble behavior is nonstationary and develops aging; that is, the transition probabilities governing the walker ensemble depend on the initial time [Eq. (32)]. The random drift induced

by the difference between the transitions probabilities lead to trajectories where the walker may persist during an entire realization with the same velocity. Nevertheless, the time intervals where this happen are characterized by a finite average (Appendix A).

Given that the transition probabilities asymptotically converge to one-half [Eq. (8)], time-averaged moments performed with infinite-time trajectories become equivalent to that of an unbiased normal random walk [Eqs. (34) and (35)]. Hence, the process is nonergodic. The vanishing of the first time-averaged moment implies that the dynamics is (asymptotically) insensitive to the bias introduced by the characteristic parameters. On the other hand, in the diffusive regime an ultraweak ergodicity breaking phenomenon occurs; that is, for the second moment ensemble and time averages differ only by a constant.

For finite-time trajectories, the time-averaged moments develop a randomness that appears in both the scaling exponents and their amplitudes (Fig. 6). This effect is induced by the intrinsic randomness of the power-law decay of the transition probabilities (Fig. 1). Departure between ensemble averages performed with finite-time trajectories (Fig. 7) and the corresponding infinite-time limit are also governed by power-law behaviors [Eqs. (42) and (43)]. No simple relation can be established between the mean asymptotic behaviors of the first two time-averaged moments (driven and undriven cases).

The studied model recovers many features that also arise in Lévy walks. While their time-averaged properties are not equivalent, the present results demonstrate that many properties of anomalous diffusive processes can also be recovered with simple globally correlated dynamics.

ACKNOWLEDGMENTS

This work was supported by Consejo Nacional de Investigaciones Científicas y Técnicas (CONICET), Argentina.

APPENDIX A: PROBABILITY OF SOJOURN TIMES

Here we obtain the probability of the sojourn times, that is, the time intervals during which the walker moves in the same direction. Equivalently, they correspond to the time during which the “velocity” is the same. Given that the walker at time t performed t_{\pm} right-left transitions, the probability of performing k successive jumps to the *right*, from the definition (3), is given by

$$P_t(k) = \prod_{i=0}^{k-1} \frac{\lambda q_+ + \mu(t_+ + i) + (1 - \mu)t_-}{t + i + \lambda} \times \frac{\lambda q_- + \mu t_- + (1 - \mu)(t_+ + k)}{t + k + \lambda}. \quad (A1)$$

The last term takes into account the beginning of a sojourn time with transitions in the opposite direction. By using the property of the Gamma function, $\Gamma(n + z)/\Gamma(z) = z(1 + z)(2 + z) \cdots (n - 1 + z)$, the previous equation becomes

$$P_t(k) = \frac{\Gamma(t + \lambda)}{\Gamma(t + \lambda + k + 1)} [\tau_- + (1 - \mu)k] \mu^k \frac{\Gamma(k + \tau_+/\mu)}{\Gamma(\tau_+/\mu)}, \quad (A2)$$

where for shortening the expression we introduced the parameters

$$\tau_{\pm} \equiv \lambda q_{\pm} + \mu t_{\pm} + (1 - \mu)t_{\mp} = \lambda q_{\pm} + \frac{1}{2}(t \pm \alpha x_t), \quad (\text{A3})$$

$\alpha = (2\mu - 1)$. The last equality straightforwardly follows from the relation (4). In this way, $P_t(k)$ depends on at which time and which position the sojourn interval begins. The structure of this dependence is simpler in the asymptotic regime $t \gg \lambda$. By using the Gamma function property $\Gamma(z + v)/\Gamma(z) \simeq z^v$ valid for $z \rightarrow \infty$, Eq. (A2) becomes

$$P_t(k) \simeq \frac{1}{(t + \lambda)^{k+1}} [\tau_- + (1 - \mu)k] \tau_+^k. \quad (\text{A4})$$

Approximating $\tau_{\pm} \simeq t w_{\pm}$ for $t \gg \lambda$, where

$$w_{\pm} \equiv \frac{1}{2} \left[1 \pm \alpha \frac{x_t}{t} \right], \quad (\text{A5})$$

($w_+ + w_- = 1$) we obtain the final expression

$$P_t(k) \simeq w_{\pm}^k w_{\mp}. \quad (\text{A6})$$

The corrections to this expression are of order $(1/t)$. On the other hand, we notice that w_{\pm} are the asymptotic transition probabilities defined in Eq. (6).

For $\mu \geq 1/2$, for increasing (decreasing) x_t the probability $P_t(k)$ increases (decreases). That is, if the particle attains larger (smaller) values of x_t the possibility of larger sojourn times in the same direction increases (decreases). This dependence of $P_t(k)$ with x_t is confirmed by its values in the boundary $x_t = \pm t$, and $x_t = 0$,

$$P_t(k) \simeq \begin{cases} (1 - \mu)\mu^k, & x_t = +t, \\ \left(\frac{1}{2}\right)^{k+1}, & x_t = 0, \\ \mu(1 - \mu)^k, & x_t = -t, \end{cases} \quad (\text{A7})$$

which in turn also clarify the role of the parameter μ in the walker realizations. Interestingly, in spite of the previous feature the average sojourn time is finite $\langle k \rangle \equiv \sum_{k=0}^{\infty} k P_t(k) \simeq w_+/(1 - w_+)$, as well as the second moment, $\langle k^2 \rangle \equiv \sum_{k=0}^{\infty} k^2 P_t(k) \simeq w_+(1 + w_+)/(1 - w_+)^2$. Straightforwardly, the same results apply for the probability of sojourn times in the opposite direction.

APPENDIX B: DOUBLE CHARACTERISTIC FUNCTION

In this appendix we obtain an exact recursive relation for the double characteristic function

$$Q(k_1, t; k_2, \tau) \equiv \langle \exp[i(k_1 x_t + k_2 x_{t+\tau})] \rangle. \quad (\text{B1})$$

It is obtained as follows. At time $\tau + 1$, it can be written as

$$\begin{aligned} & Q(k_1, t; k_2, \tau + 1) \\ &= \left\langle \exp[i(k_1 x_t + k_2 x_{t+\tau})] \sum_{\sigma=\pm 1} e^{ik_2 \sigma} \mathcal{T}(\sigma_1, \dots, \sigma_{t+\tau} | \sigma) \right\rangle. \end{aligned} \quad (\text{B2})$$

Here we have taken into account that the random variable $\sigma_{t+\tau+1}$ is chosen in agreement with the transition probability $\mathcal{T}(\sigma_1, \dots, \sigma_{t+\tau} | \sigma_{t+\tau+1})$. Notice that the ensemble average $\langle \dots \rangle$ includes all possible random values of $\{\sigma_i\}_{i=1}^{t+\tau}$, which

in turn define all possible realizations of x_t and $x_{t+\tau}$. From Eq. (3), we get

$$\begin{aligned} Q_{t,\tau+1} &= \frac{1}{t + \tau + \lambda} \left[\lambda Q_{t,\tau} \sum_{\sigma=\pm 1} q_{\sigma} e^{ik_2 \sigma} \right. \\ &\quad \left. + \sum_{\sigma=\pm 1} \langle \exp[i(k_1 x_t + k_2 x_{t+\tau})] U_{t+\tau}^{\sigma} \rangle e^{ik_2 \sigma} \right], \end{aligned} \quad (\text{B3})$$

where the change of notation $Q(k_1, t; k_2, \tau) \rightarrow Q_{t,\tau}$ was introduced for shortening the expression. Furthermore, the random function $U_{t+\tau}^{\sigma}$ is defined as

$$U_t^{\pm} \equiv \mu t_{\pm} + (1 - \mu)t_{\mp}, \quad (\text{B4})$$

which due to the relation $t_{\pm} = (t \pm x_t)/2$ [Eq. (4)] can be rewritten as $U_t^{\pm} = (t \pm \alpha x_t)/2$. Using that

$$\frac{\partial Q_{t,\tau}}{\partial k_2} = i \langle x_{t+\tau} \exp[i(k_1 x_t + k_2 x_{t+\tau})] \rangle, \quad (\text{B5})$$

jointly with the normalization condition $q_+ + q_- = 1$, after some algebra, from Eq. (B3) it follows the closed recursive relation

$$\begin{aligned} Q_{t,\tau+1} &= \cos(k_2) Q_{t,\tau} + i \lambda \delta q \frac{\sin(k_2)}{(t + \tau + \lambda)} Q_{t,\tau} \\ &\quad + \alpha \frac{\sin(k_2)}{(t + \tau + \lambda)} \frac{\partial Q_{t,\tau}}{\partial k_2}, \end{aligned} \quad (\text{B6})$$

where $\alpha = (2\mu - 1)$, and $\delta q = (q_+ - q_-)$. By differentiation with respect to k_1 and k_2 the recursive relations presented in Sec. III follows straightforwardly.

APPENDIX C: APPROXIMATION FOR THE ENSEMBLE TIME-AVERAGED MOMENTS

Here we show the procedure to obtain the asymptotic behavior of the time-averaged moments $\langle \delta_{\kappa}(t, \Delta) \rangle$. Their exact expressions, Eqs. (38) and (39), have the following structure:

$$F(t, \Delta) = \frac{1}{t - \Delta} \sum_{t'=0}^{t-\Delta} f(t', \Delta). \quad (\text{C1})$$

The goal is to approximate $F(t, \Delta)$ at large time scales, $t \gg \Delta$, given that we have an exact expression for $f(t', \Delta)$ written in terms of the ensemble moments $\langle x_t \rangle$, $\langle x_t^2 \rangle$, and the correlation $\langle x_{t'+\Delta} x_{t'} \rangle$.

Defining the variable $\varepsilon \equiv \Delta/t$, the scaled time $\tau \equiv t'/t$, and $d\tau \equiv 1/t$, the previous general expression can be rewritten as

$$F(t, t\varepsilon) = \frac{1}{1 - \varepsilon} \sum_{\tau=0}^{1-\varepsilon} f(t\tau, t\varepsilon) d\tau. \quad (\text{C2})$$

In this expression $d\tau = 1/t \ll 1$, and consistently $\tau = t'/t$ can be considered as a real continuous variable. Therefore, we can approximate the sum by an integral,

$$F(t, \Delta) \simeq \frac{1}{1 - \varepsilon} \int_0^{1-\varepsilon} f(t\tau, t\varepsilon) d\tau. \quad (\text{C3})$$

In addition, given that only the asymptotic regime is of interest, before performing this integral $f(t\tau, t\varepsilon)$ can be approximated

by its asymptotic behavior. Posteriorly, the integral can be expanded in the parameter ε . This procedure leads to the approximations given in Eqs. (42) and (43).

The parameters of Eq. (43) are

$$a = \frac{(1-\mu)(1-2\mu)}{4\mu-3} \{3 - 2H[2(1-\mu)]\}, \quad (C4)$$

where $H[x] = \gamma + \psi(x-1)$, where γ is the Euler constant and $\psi(x)$ is the digamma function,

$$b = \frac{2}{4\mu-3} [(1-\mu)(2\mu-1)] \quad (C5)$$

and

$$c = \frac{(1-2\mu)^2}{(4\mu-3)^2} \frac{\Gamma(1+\lambda)}{\Gamma(4\mu-2+\lambda)}, \quad (C6)$$

while

$$d = \frac{-1}{(4\mu-3)} \frac{\Gamma(1+\lambda)}{\Gamma(4\mu-2+\lambda)} \times \left[\frac{1}{4\mu-1} + \frac{2^{1-4\mu}}{\sqrt{\pi}} \Gamma\left(\frac{1}{2} - 2\mu\right) \Gamma(2\mu) \right]. \quad (C7)$$

-
- [1] V. Zaburdaev, S. Denisov, and J. Klafter, Lévy walks, *Rev. Mod. Phys.* **87**, 483 (2015).
- [2] H. Scher and E. W. Montroll, Anomalous transit-time dispersion in amorphous solids, *Phys. Rev. B* **12**, 2455 (1975); J. Klafter, A. Blumen, and M. F. Shlesinger, Stochastic pathway to anomalous diffusion, *Phys. Rev. A* **35**, 3081 (1987); T. Geisel, J. Nierwetberg, and A. Zacherl, Accelerated Diffusion in Josephson Junctions and Related Chaotic Systems, *Phys. Rev. Lett.* **54**, 616 (1985); M. F. Shlesinger, B. J. West, and J. Klafter, Lévy Dynamics of Enhanced Diffusion: Application to Turbulence, *ibid.* **58**, 1100 (1987).
- [3] G. Zumofen and J. Klafter, Scale-invariant motion in intermittent chaotic systems, *Phys. Rev. E* **47**, 851 (1993); Power spectra and random walks in intermittent chaotic systems, *Phys. D* **69**, 436 (1993).
- [4] G. Trefán, E. Floriani, B. J. West, and P. Grigolini, Dynamical approach to anomalous diffusion: Response of Lévy processes to a perturbation, *Phys. Rev. E* **50**, 2564 (1994).
- [5] I. M. Sokolov and R. Metzler, Towards deterministic equations for Lévy walks: The fractional material derivative, *Phys. Rev. E* **67**, 010101(R) (2003).
- [6] M. Magdziarz, W. Szczotka, and P. Zebrowski, Langevin picture of Lévy walks and their extensions, *J. Stat. Phys.* **147**, 74 (2012).
- [7] Y. He, S. Burov, R. Metzler, and E. Barkai, Random Time-Scale Invariant Diffusion and Transport Coefficients, *Phys. Rev. Lett.* **101**, 058101 (2008).
- [8] A. Lubelski, I. M. Sokolov, and J. Klafter, Nonergodicity Mimics Inhomogeneity in Single Particle Tracking, *Phys. Rev. Lett.* **100**, 250602 (2008).
- [9] G. Bel and I. Nemenman, Ergodic and nonergodic anomalous diffusion in coupled stochastic processes, *New J. Phys.* **11**, 083009 (2009).
- [10] K. Burnecki and A. Weron, Fractional Lévy stable motion can model subdiffusive dynamics, *Phys. Rev. E* **82**, 021130 (2010).
- [11] A. Fulinski, Anomalous diffusion and weak nonergodicity, *Phys. Rev. E* **83**, 061140 (2011).
- [12] Y. Meroz, I. M. Sokolov and J. Klafter, Subdiffusion of mixed origins: When ergodicity and nonergodicity coexist, *Phys. Rev. E* **81**, 010101(R) (2010); F. Thiel and I. M. Sokolov, Weak ergodicity breaking in an anomalous diffusion process of mixed origins, *ibid.* **89**, 012136 (2014).
- [13] T. Albers and G. Radons, Subdiffusive continuous-time random walks and weak ergodicity breaking analyzed with the distribution of generalized diffusivities, *Eur. Phys. Lett.* **102**, 40006 (2013).
- [14] A. G. Cherstvy, A. V. Chechkin, and R. Metzler, Anomalous diffusion and ergodicity breaking in heterogeneous diffusion processes, *New J. Phys.* **15**, 083039 (2013); A. G. Cherstvy and R. Metzler, Non-ergodicity, fluctuations, and criticality in heterogeneous diffusion processes, *Phys. Rev. E* **90**, 012134 (2014); Ergodicity breaking, ageing, and confinement in generalized diffusion processes with position and time dependent diffusivity, *J. Stat. Mech.* (2015) P05010.
- [15] O. Peters, Ergodicity Breaking in Geometric Brownian Motion, *Phys. Rev. Lett.* **110**, 100603 (2013).
- [16] P. Massignan, C. Manzo, J. A. Torreno-Pina, M. F. G.- Parajo, M. Lewestein, and G. J. Lapeyre, Jr., Nonergodic Subdiffusion from Brownian Motion in an Inhomogeneous Medium, *Phys. Rev. Lett.* **112**, 150603 (2014).
- [17] A. Godec, A. V. Chechkin, E. Barkai, H. Kantz, and R. Metzler, Localization and universal fluctuations in ultraslow diffusion processes, *J. Phys. A* **47**, 492002 (2014).
- [18] H. Safdari, A. G. Cherstvy, A. V. Chechkin, F. Thiel, I. M. Sokolov, and R. Metzler, Quantifying the non-ergodicity of scaled Brownian motion, *J. Phys. A* **48**, 375002 (2015); H. Safdari, A. V. Chechkin, G. R. Jafari, and R. Metzler, Aging scaled Brownian motion, *Phys. Rev. E* **91**, 042107 (2015).
- [19] Y. Lanoiselée and D. S. Grebenkov, Revealing nonergodic dynamics in living cells from a single particle trajectory, *Phys. Rev. E* **93**, 052146 (2016).
- [20] T. Akimoto and E. Yamamoto, Distributional behaviors of time-averaged observables in the Langevin equation with fluctuating diffusivity: Normal diffusion but anomalous fluctuations, *Phys. Rev. E* **93**, 062109 (2016).
- [21] C. Manzo and M. F. G.- Parajo, A review of progress in single particle tracking: From methods to biophysical insights, *Rep. Prog. Phys.* **78**, 124601 (2015); S. Burov, J.-H. Jeon, R. Metzler, and E. Barkai, Single particle tracking in systems showing anomalous diffusion: The role of weak ergodicity breaking, *Phys. Chem. Chem. Phys.* **13**, 1800 (2011).
- [22] H. Safdari, A. G. Cherstvy, A. V. Chechkin, A. Bodrova, and R. Metzler, Aging underdamped scaled Brownian motion: Ensemble- and time-averaged particle displacements, nonergodicity, and the failure of the overdamping approximation, *Phys. Rev. E* **95**, 012120 (2017).
- [23] A. Godec and R. Metzler, Finite-Time Effects and Ultraweak Ergodicity Breaking in Superdiffusive Dynamics, *Phys. Rev. Lett.* **110**, 020603 (2013).
- [24] D. Froemberg and E. Barkai, Time-averaged Einstein relation and fluctuating diffusivities for the Lévy walk,

- Phys. Rev. E* **87**, 030104(R) (2013); Random time averaged diffusivities for Lévy walks, *Eur. Phys. J. B* **86**, 331 (2013).
- [25] A. Godec and R. Metzler, Linear response, fluctuation-dissipation, and finite-system-size effects in superdiffusion, *Phys. Rev. E* **88**, 012116 (2013).
- [26] D. Froemberg and E. Barkai, No-go theorem for ergodicity and an Einstein relation, *Phys. Rev. E* **88**, 024101 (2013).
- [27] T. Akimoto, Distributional Response to Biases in Deterministic Superdiffusion, *Phys. Rev. Lett.* **108**, 164101 (2012); Generalization of the Einstein relation for single trajectories in deterministic subdiffusion, *Phys. Rev. E* **85**, 021110 (2012).
- [28] V. Tejedor and R. Metzler, Anomalous diffusion in correlated continuous-time random walks, *J. Phys. A* **43**, 082002 (2010); M. Magdziarz, R. Metzler, W. Szczotka, and P. Zebrowski, Correlated continuous-time random walks in external force fields, *Phys. Rev. E* **85**, 051103 (2012).
- [29] G. M. Schütz and S. Trimper, Elephants can always remember: Exact long-range memory effects in a non-Markovian random walk, *Phys. Rev. E* **70**, 045101(R) (2004).
- [30] H. Kim, Anomalous diffusion induced by enhancement of memory, *Phys. Rev. E* **90**, 012103 (2014).
- [31] R. Kürsten, Random recursive trees and the elephant random walk, *Phys. Rev. E* **93**, 032111 (2016).
- [32] V. M. Kenkre, Analytic formulation, exact solutions, and generalizations of the elephant and the Alzheimer random walks, [arXiv:0708.0034](https://arxiv.org/abs/0708.0034).
- [33] J. C. Cressoni, M. A. A. da Silva, and G. M. Viswanathan, Amnestically Induced Persistence in Random Walks, *Phys. Rev. Lett.* **98**, 070603 (2007); A. S. Ferreira, J. C. Cressoni, G. M. Viswanathan, and M. A. Alves da Silva, Anomalous diffusion in non-Markovian walks having amnestically induced persistence, *Phys. Rev. E* **81**, 011125 (2010); J. C. Cressoni, G. M. Viswanathan, and M. A. A. da Silva, Exact solution of an anisotropic 2D random walk model with strong memory correlations, *J. Phys. A* **46**, 505002 (2013).
- [34] M. A. A. da Silva, J. C. Cressoni, G. M. Schütz, G. M. Viswanathan, and S. Trimper, Non-Gaussian propagator for elephant random walks, *Phys. Rev. E* **88**, 022115 (2013).
- [35] C. F. Coletti, R. Gava, and G. M. Schütz, Central limit theorem for the elephant random walk, [arXiv:1608.01662](https://arxiv.org/abs/1608.01662) [cond-math.stat-mech].
- [36] E. Baur and J. Bertoin, Elephant random walks and their connection to Pólya-type urns, *Phys. Rev. E* **94**, 052134 (2016).
- [37] F. N. C. Paraan and J. P. Esguerra, Exact moments in a continuous-time random walk with complete memory of its history, *Phys. Rev. E* **74**, 032101 (2006).
- [38] N. Kumar, U. Harbola, and K. Lindenberg, Memory-induced anomalous dynamics: Emergence of diffusion, subdiffusion, and superdiffusion from a single random walk model, *Phys. Rev. E* **82**, 021101 (2010); U. Harbola, N. Kumar, and K. Lindenberg, Memory-induced anomalous dynamics in a minimal random walk model, *ibid.* **90**, 022136 (2014).
- [39] D. Boyer and J. C. Romo-Cruz, Solvable random-walk model with memory and its relations with Markovian models of anomalous diffusion, *Phys. Rev. E* **90**, 042136 (2014).
- [40] A. A. Budini, Inhomogeneous diffusion and ergodicity breaking induced by global memory effects, *Phys. Rev. E* **94**, 052142 (2016).
- [41] B. J. West, E. L. Geneston, and P. Grigolini, Maximizing information exchange between complex networks, *Phys. Rep.* **468**, 1 (2008); J. P. Bouchaud and A. Georges, Anomalous diffusion in disordered media: Statistical mechanisms, models and physical applications, *ibid.* **195**, 127 (1990).
- [42] J. H. P. Schulz, E. Barkai, and R. Metzler, Aging Renewal Theory and Application to Random Walks, *Phys. Rev. X* **4**, 011028 (2014).
- [43] M. Magdziarz and T. Zorawik, Aging ballistic Lévy walks, *Phys. Rev. E* **95**, 022126 (2017).
- [44] A. A. Budini, Weak ergodicity breaking induced by global memory effects, *Phys. Rev. E* **94**, 022108 (2016).
- [45] A. Rebenshtok and E. Barkai, Weakly non-ergodic statistical physics, *J. Stat. Phys.* **133**, 565 (2008); Distribution of Time-Averaged Observables for Weak Ergodicity Breaking, *Phys. Rev. Lett.* **99**, 210601 (2007); G. Bel and E. Barkai, Stochastic Ergodicity Breaking: A Random Walk Approach, *ibid.* **94**, 240602 (2005).
- [46] A. A. Budini, Central limit theorem for a class of globally correlated random variables, *Phys. Rev. E* **93**, 062114 (2016).